Polyolefin/Polyether Alternated Copolymers: Silyl-Modified Polymers as Promising Monocomponent Precursors to Adhesives

Cyril Chauveau, Stéphane Fouquay, Guillaume Michaud, Frédéric Simon,
Jean-Francois Carpentier, Sophie M. Guillaume

Polyolefin/Polyether Alternated Copolymers: Silyl-Modified Polymers as Promising Monocomponent Precursors to Adhesives

Cyril Chauveau,[a] Stéphane Fouquay,[b] Guillaume Michaud,[c] Frédéric Simon,[c] Jean-François Carpentier (ORCID: 0000-0002-9160-7662),[a,*] and Sophie M. Guillaume (ORCID: 0000-0003-2917-8657)[a,*]

[a] Univ Rennes, CNRS, ISCR (Institut des Sciences Chimiques de Rennes) – UMR 6226, F-35000 Rennes, France

[b] BOSTIK S.A., 420 rue d'Estienne d'Orves, 92705 Colombes Cedex, France

[c] BOSTIK, ZAC du Bois de Plaisance, 101, Rue du Champ Cailloux, F-60280 Venette, France

---

[*] Corresponding authors: jean-francois.carpentier@univ-rennes1; sophie.guillaume@univ-rennes1.fr

Graphical abstract

COE Polyether diacrylate Bis(trialkoxysilyl) alkene CTA

ROIMP/CM Ru catalyst

Polyether/polyolefin SMP

Polycondensation moisture

Cross-linked polyether/polyolefin SMP

SMP-based adhesive
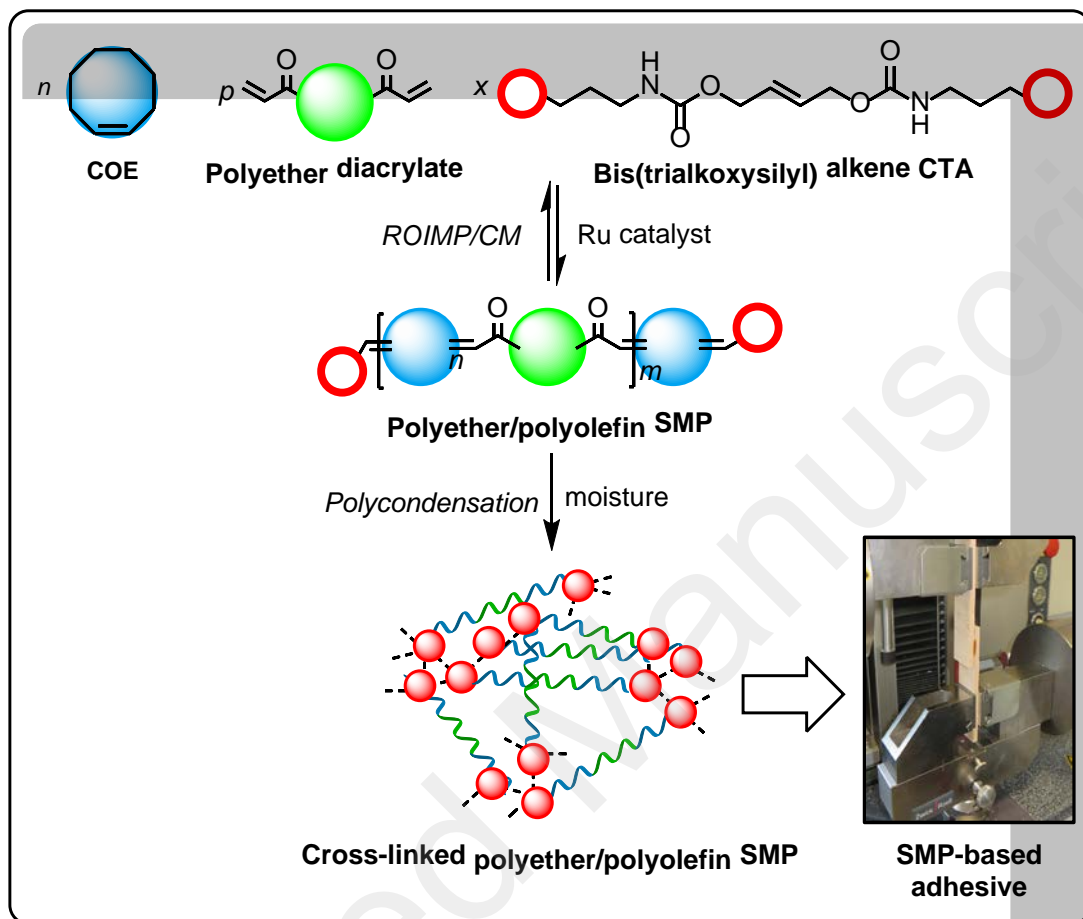
Abstract

α,ω-Bis(trialkoxysilyl) telechelic polyether/polyolefin copolymers were synthesized and evaluated as <u>monocomponent</u> adhesive precursors. The Ru-catalyzed tandem ring-opening insertion-metathesis polymerization (ROIMP) and cross metathesis (CM) reactions in the presence of a bis(trialkoxysilyl)alkene as chain-transfer agent (CTA) were first explored towards the synthesis of such silyl-modified polymers (SMPs). The one-pot, two-step ROIMP/CM of cyclooctene (COE) and poly(propyleneglycol) diacrylate (PPG$^{(*)}$) with $\{(EtO)_3Si(CH_2)_3NHC(O)OCH_2CH=\}_2$ (CTA^{Et}) catalyzed by Grubb's 2nd generation catalyst (Method II) successfully enables the preparation of α,ω-[(EtO)$_3$Si]$_2$-PCOE/PPG$^{(*)}$ alternated copolymers, isolated in 10−100 g. The polyether/polyolefin copolymers were thoroughly characterized by SEC, 1D and 2D NMR, and FTIR spectroscopies and mass spectrometry analyses. The good thermal stability and rheofluidifying profile of the PCOE/PPG* copolymers are maintained following their catalyzed moisture-curing, as revealed by TGA, DSC and rheology. The corresponding siloxane cross-linked copolymers then demonstrate strain-at-break, elongation-at-break and wood-adhesion properties greater than those of the benchmarked SMP reference from Bostik, namely Polyvest E100 (strain-at-break on wood up to 4.0 vs 2.6 MPa, respectively). These characteristics can be tuned according to the PCOE/PPG* ratio, and also revealed significantly better than the ones of our previously reported alike siloxane cross-linked PCOE/PPG* copolymers similarly prepared yet from a one-pot, one-step ROIMP/CM approach (Method I). Such polyolefin/polyether monocomponent SMPs are thus promising adhesive precursors.

Introduction

Common silyl-modified polymers (SMPs) include polyolefins, polyurethanes (PUs), polyethers or polyacrylates bearing alkoxysilyl functional groups. They are mainly exploited in the coatings, adhesives, sealants and elastomers (CASE) industry.[1,2,3,4] Indeed, SMPs can harden upon formation of a dense polysiloxane 3D network through the polycondensation of their alkoxysilyl groups with moisture. SMPs also provide an alternative to toxic isocyanate-terminated moisture-curable PUs. Furthermore, they are valued for their good adhesion to a wide range of substrates (e.g. glass, plastics and metals), good resistance to temperature and UV irradiation, foaming-free, fast and controlled curing, lack of strong odor or staining, great durability, and reduced health issues.[5,6,7] The adhesive market is a huge target with almost 14 million tons of adhesives consumed worldwide and a $50 billion turnover for the global adhesive market in 2019.[8] In addition to binding substrates, adhesives provide many other valuable advantages including protection to corrosion, impact and grinding, flexibility between the substrates, lessening of noise and vibrations, reduction of the final weight and cost of the material compared to mechanical binding parts (screws, rivets,..), and insulation of electronic parts.[9] Given such a vast market of adhesives which are nowadays part of our daily life, and taking into account that an efficient adhesive is a polymer in a liquid state showing a high chemical affinity with the substrates to bound, and prone to harden into a strong solid upon curing, SMPs are thus both industrially and environmentally attractive since they provide water-based and solvent free monocomponent adhesives.[1-9]

Polyolefin-based SMPs (SMPOs) are valuable for their ability to adhere to non-polar and non-porous olefinic surfaces. SMPOs have been traditionally prepared from chemical modification (either *in situ* functionalization or post-polymerization functionalization) routes, or more valuably from olefin metathesis (self-metathesis, cross metathesis (CM), ring-opening metathesis polymerization (ROMP) and acyclic diene metathesis (ADMET)

polymerization) approaches. In particular, the tandem ROMP/CM of a cyclic olefin, in the presence of a symmetric di(alkoxysilyl) functional alkene chain transfer agent (CTA), appears as a valuable, mild and rather highly selective route to SMPOs.[10] The functional olefinic CTA undergoes CM reactions with the internal C=C bonds throughout the growing polyolefin chains or with the active catalyst moiety bearing the functional group, thus advantageously giving α,ω-chain-end difunctional polyolefins.[11,12,13,14,15,16] In this regard, we have recently reported a range of SMPOs based on different cyclic olefins prepared by ROMP/CM, catalyzed by some ruthenium complexes in the presence of several bis(trialkoxysilyl)alkene CTAs.[17,18,19,20] Also, Wagener and co-workers previously reported the preparation by ADMET polymerization of bis(dimethoxymethylsilyl) telechelic polyether/carbosiloxane copolymers, which displayed enhanced elasticity and adhesion properties thanks to the incorporation of some oligo(oxyethylene) segments within the polyolefin.[21,22,23,24,25] With the objective to expand the thermo-mechanical and adhesion properties of our SMPOs, we thus tackled the incorporation of "soft" polyether segments within a "rigid" polyolefin backbone.[26]

Alternated copolyolefins have been reported by ROMP by several research groups.[27,28,29,30,31] However, the design of specific asymmetric catalysts was then required in order to achieve such an alternated topology.[32] Additionally, Grubbs, Choi and co-workers reported the first synthesis of alternated olefin-based copolymers through an original metathesis approach, namely the ring-opening insertion metathesis polymerization (ROIMP) of cyclic olefins and diacrylates (Scheme S1).[33,34] It was then demonstrated that the fast ROMP of the cyclic olefin first occurs, followed by the slow and progressive insertion of the diacrylate segment within the polymer chains. The ROIMP is thermodynamically driven by the selective bond formation between the cycloalkene and the diacrylate (Table S1). Since the self-metathesis of two electron-deficient acrylate functions is highly unfavorable,[35] the selective bond formation between the diacrylate and the olefin takes place. Provided a

5

stoichiometric loading in monomers is used, this ensures the formation of highly alternated polymers. Cyclopentene, cycloheptene, cyclododecene, cyclooctene (COE), and COE derivatives were thus copolymerized with alkyl, aryl or diethylene glycol diacrylates. High conversions were obtained for their copolymerization with typical 7- and 8-membered cycloolefins and cyclododecene, with up to 98.5% alternation, high molar mass and moderate dispersity values (Table S1).[33] The newly established ROIMP route thus revealed particularly interesting for its tolerance to virtually any diacrylate (macro)molecules, thereby paving the way to the incorporation of functional groups (*i.e.* ether or aromatic segments) within polyolefins (Table S1, entries 6,7). The ADMET variant of the ROIMP, sometimes referred to as the alternating diene metathesis polycondensation (ALTMET, Scheme S2), was also described along with an example of tandem ROMP/ADMET.[36,37,38,39,40] However, regardless of the improvements achieved during the optimization of this latter approach, the operating conditions (especially the catalyst loading and the reaction temperature) were not suitable for a metathesis polymerization. Noteworthy, to the best of our knowledge, the innovative ROIMP reaction has not been further explored, and there is not precedent of ROIMP or ALTMET performed in the presence of a CTA towards the synthesis of telechelic polyolefins.

We thus report herein on the incorporation of polyether segments within a PCOE backbone, through the ROIMP/CM strategy using commercially available diacrylate end-capped poly(propyleneglycol). Our initial report described the synthesis of α,ω-[Si(OEt)$_3$]$_2$-PCOE/PPG* by a *one-pot, one-step* tandem ROIMP/CM of COE and PPG* with CTA^{Et} catalyzed by G2 in a concentrated reaction medium, along with the thermomechanical and adhesives properties of (cured) SMP copolymers.[26] The present investigations further explore different routes and operating conditions to optimize the synthetic pathway, especially in terms of conversion in each reagent and suitability to access significant amounts of copolymers (Schemes 1, S3−S5). Studies are first based on the simpler tri(propyleneglycol)

diacrylate polyether (PPG) model and next complemented with the industrially-relevant poly(propyleneglycol$_{31}$diurethane) diacrylate (PPG*). These various synthetic strategies demonstrate that one-pot approaches based on the tandem ROIMP/CM of COE and PPG* with CTA^{Et} catalyzed by G2 (two-step Method II – herein established – and one-step Method I – previously reported –[26]) are the most suitable pathways towards the large-scale preparation of such polyolefin/polyether SMP materials. The thermo-mechanical, rheological and adhesive properties of the thus herein synthesized (Method II), and of the subsequently cured corresponding new PCOE/PPG* SMP materials, are next examined to probe in particular the impact of the polyether segments' length and the content of trialkoxysilyl moieties. Comparison of these characteristics, to those of alike siloxane cross-linked PCOE/PPG* materials obtained from the one-step Method I as previously reported,[26] and benchmarking with the commercial adhesive Polyvest E100, reveal improved thermal, mechanical and especially, adhesives features of the new SMPs established in the present work from the two-step ROIMP/CM Method II.

Experimental Section

Materials.

All catalytic experiments were performed under inert atmosphere (argon, < 3 ppm O$_2$) using standard Schlenk line and glove box techniques. Grubbs' 2nd generation catalyst, ([(IMesH$_2$)(Cy$_3$P)RuCl$_2$(=CHPh)], G2, Aldrich) was used as received. Cyclooctene (COE) was purchased from ACROS, and dried and distilled over CaH$_2$ before use. Bis(acrylate)tripropyleneglycol referred to as PPG, was kindly provided by Sartomer, and purified by flash chromatography over silica (CH$_2$Cl$_2$) and stored over 3Å molecular sieves prior to use (Figure S1). The diacrylate end-capped poly(propyleneglycol$_{31}$diurethane) (PPG[C$_6$H$_3$(Me)(NHC(O))$_2$] diacrylate, PPG*; Figure S2; the SEC trace shows three main

7

peaks at $M_{n,SEC}$ = 3500 (59%), 7200 (24%), 12 000 g.mol^{-1} (13%) with $Đ_M$ = 1.0 for each of them, corresponding to three distinct values of repeating units within PPG*, namely n = 1, 2 and 3, respectively), and Polyvest E100 (Evonik, $M_{n,SEC}$ = 5700 g.mol^{-1}) were kindly supplied by Bostik and used as received (Figure S3). (*E*)-But-2-ene-1,4-diyl bis((3-(triethoxysilyl)propyl)carbamate) (CTA^{Et}) was synthesized as previously described.[17–20,26]

Instrumentation and measurements.

^{1}H (500, 400 MHz) and ^{13}C{^{1}H} (125, 100 MHz) NMR spectra were recorded on Bruker Avance AM 500 and AM 400 spectrometers at 23 °C in CDCl$_3$. Chemical shifts (δ) are reported in ppm and were referenced internally relative to tetramethylsilane (δ 0 ppm) using the residual ^{1}H and ^{13}C solvent resonances of the deuterated solvent.

Monomer conversions were determined from ^{1}H NMR spectra of the crude polymer sample, from the integration (Int.) ratio Int.$_{Polymer}$/[Int.$_{Polymer}$ + Int.$_{monomer}$], using the methine hydrogens (–C*H*=C*H*– : δ 5.30, 5.66 ppm (PCOE, COE)). Quantitative COE conversion was thus established by ^{1}H NMR analysis. The typical ^{1}H and ^{13}C NMR spectra of the final copolymers evidenced the presence of four different chain-ends (i.e. functional groups (FG), Scheme 1), namely trialkoxysilyl chain-ends originating from the CTA (H^{a-i}), acrylate (Acryl., H^{l,m}) and vinyl (Vinyl, H^{j,k}) chain-ends arising from the reaction of PPG$^{(*)}$ with COE units, and isomerized (Isom., H^{n-p}) chain-ends issued from the internal isomerization of vinyl groups (Figure 1). Quantitative analyses of the ^{1}H NMR spectra thus enabled to determine the conversion in CTA^{Et} (δ 4.56 ppm, C(O)OC*H*^{g}$_2$C*H*=C*H* CTA^{Et}, vs δ 4.48,4.61 C*H*^{g}$_2$OC(O)NH chain-end), and the content in acrylate (Acryl.; δ 6.22 ppm C*H*^{l}$_2$=CHC(O) vs 6.97 ppm C*H*^{H}$_2$=CHC(O)), Si(OEt)$_3$ (δ 0.65 ppm, (OEt)$_3$SiC*H*^{c}$_2$CH$_2$)), vinyl (δ 5.78 ppm, C*H*^{j}$_2$=CHCH$_2$) and isomerized (Isom.; δ 1.64 ppm, CH=CHC*H*^{n}$_3$) chain end-groups, from their relative intensity (Figure 1). Assuming the absence of any unreacted PPG$^{(*)}$ (unreacted

8

PPG[(*)] and acrylate chain-ends have isochronous NMR resonances), the relative content of these various chain-ends was determined by comparison of H^c, H^g, H^j, H^n and H^l, using a deconvolution method for overlapping signals (Tables 1,2,S5,S6,S7). Of note, the ethylene formed during the metathesis reactions was immediately flushed away either by a flow of argon of by vacuum. The amount of ethylene released was thus indirectly determined by ^{1}H NMR monitoring of vinyl chain-ends consumption since ethylene was formed by self-metathesis of vinyl chain-ends during the reaction (comparison of H^H, H^j and H^m) (Figure 1; Schemes S6,S7,S8).[41] Experimental molar mass values could not be reliably estimated from NMR spectra due to the latter's complexity and especially because of the overlap of several characteristic signals.

The average molar mass ($M_{n,SEC}$) and dispersity ($Đ_M = M_w/M_n$) values of the freshly prepared polymer samples (at most within one week following their synthesis unless otherwise stated; stored under argon following synthesis and analyses) were determined by size exclusion chromatography (SEC) in THF at 30 °C (flow rate = 1.0 mL.min^{-1}) on a Polymer Laboratories PL50 apparatus equipped with a refractive index detector and a set of two ResiPore PLgel 3 μm MIXED-E 300 × 7.5 mm columns. The polymer samples were dissolved in THF (2 mg.mL^{-1}). All elution curves were calibrated with twelve monodisperse polystyrene standards (M_n range = 580–380,000 g.mol^{-1}). $M_{n,SEC}$ values of polymers were uncorrected for their possible difference in hydrodynamic volume in THF vs polystyrene. The SEC traces of the copolymers all exhibited a monomodal and symmetric peak.

FTIR spectra of the polymers were acquired (16 scans) with a resolution of 4 cm^{-1} on a Shimadzu IRAffinity-1 equipped with an ATR module.

Thermogravimetric analyses (TGA) were performed on a Mettler Toledo TGA/DSC1 by heating polymer samples at a rate of 10 °C.min^{-1} from +25 °C to +500 °C in a dynamic nitrogen atmosphere (flow rate = 50 mL.min^{-1}).

Differential scanning calorimetry (DSC) analyses were performed with a Setaram DSC 131 apparatus calibrated with indium, at a rate of 10 °C min^{-1}, under a continuous flow of helium (25 mL.min^{-1}), using aluminum capsules. The thermograms were recorded according to the following cycles: −100 to 150 °C at 10 °C min^{-1}; 150 to −100 °C at 10 °C min^{-1}.

The apparent viscosity of the SMPs was measured with an ARES G2 planar viscosimeter equipped with a plate-plate geometry, at a speed gradient of 0.01 s^{-1} over a shear rate range from 0.01 to 100.s^{-1}. At each imposed shear rate, the apparent viscosity was determined in the steady state regime. The operating temperature was fixed at 30 or 60 ± 0.3 °C. For each sample, the viscosimetric test duration was 5 min. The polymer sample was introduced in between two flat plates inside an oven. A motor was spinning the superior plate, which was in turn spinning the polymer sample. Shear rate ($γ$, with $γ = v/h$, v the velocity of the plate (m.s^{-1}), h the distance between the two plates (m)) was gradually increased from $γ =$ 0.01 to 500 s^{-1}. During the measurement, h was kept constant at 0.5 mm. The viscosity of the sample in function of $γ$ was then calculated from the formula:

$$\eta = \frac{F}{\gamma \times A} \ (\mathrm{Pa.\,s})$$

with F = the force applied to the upper plate by the polymer in response to the movement of rotation (N), and A = the contact area between the sample and the plate (m^2). Noteworthy, rheofluidifying polymers are particularly adapted to adhesive applications. They can be easily formulated with catalyst and other additives, they remain homogenous for long periods of time, and their application on surfaces is easy.

Dynamic mechanical analysis (DMA) were performed on a MCR302 Rheometer (Anton Paar) equipped with a CTD450 furnace. An extensional tool was used to make DMA tensile tests. The films were then clamped between the two parallel rolls. The analyzed

sample length was 20 mm. To avoid sample slipping during measurements, rough rolls were used. Adhesive films were cut in small rectangular pieces (ca. 30 x 8.5 m; thickness ca. 150 μm). Films were heated from −90 to +150 °C at 2 ° min^{-1} under nitrogen flow. Linear domains were first measured for each sample on the whole temperature range. Then, the method parameters were adjusted if samples were different from one another. Most of the time, oscillation parameters were fixed at 1 Hz, with a strain amplitude evolving from 0.1 to 0.3 %, between −90 and +150 °C.

CM of PPG$^{(*)}$ with several bis(trialkoxysilyl)alkene CTAs using various catalytic systems. Refer to Supporting Information for details (Scheme S3, Tables S2–S3, Figures S4–S13).

One-pot or two-pot, two-step ROMP/CM of COE catalyzed by G2 in the presence of CTA^{Et} and IM of PPG. Refer to the Supporting information for details (Scheme S4, Tables S4–S5).

One-pot, one-step ROIMP/CM of COE and PPG catalyzed by G2 in the presence of CTA^{Et}. Refer to the Supporting information for details (Scheme S5, Table S6, Figure S14).

One-pot, two-step ROIMP of COE and PPG catalyzed by G2 and CM in the presence of CTA^{Et} - Method II. The ROIMP of COE and PPG catalyzed by G2 was performed as previously reported with PPG*, yet in the absence of a CTA, in CH$_2$Cl$_2$ at 40 °C during 24 h (Scheme 1, Table 1).[26] The subsequent CM in the presence of CTA^{Et} was next performed *in situ* (one-pot) upon addition of CTA^{Et} to the reaction mixture at 40 °C during 24 h, as for a classical CM reaction (Scheme 1, Table 2).[20] The reaction times were not optimized. Refer to the Supporting information for details. Note that the amount of cyclic polymers could not be determined following the procedure previously reported.[18–20] Indeed, the recovered α,ω-[Si(OEt)$_3$]$_2$PCOE/PPG copolymers were too reactive to be successfully trapped onto acidified silica during their elution aimed to provide only cyclic copolymers.

One-pot, two-step ROIMP of COE and PPG* catalyzed by G2 and CM in the presence of CTA^{Et}: Large-scale synthesis - Method II. Practically, the ROIMP/CM of COE and PPG* catalyzed by G2 followed by the CM with CTA^{Et} was performed *in situ* (one-pot) as just described above for PPG (Scheme 1), with the following scale-up modifications. Ten individual batches of 10 g each were prepared so as to avoid scaling-up issues inherent to the preparation of 100 g at once. Thus, two-third of the required amount of G2 were sequentially introduced in four portions separated by 1 h in the ROIMP step 1, and the last 1/3rd was then introduced at once during the CM step 2. The 10 batches were next mixed together, and CH_2Cl_2 was then distilled out under vacuum raising the temperature from 40 °C to 70 °C to ultimately give a brownish highly viscous liquid (Table S7, entries 1−3; each entry thus corresponds to ca. 100 g of copolymer sample recovered from 10 individual two-step ROIMP/CM experiments) (Figures S15−S27).

One-pot, one-step ROIMP/CM of COE and PPG* catalyzed by G2 in the presence of CTA^{Et}: Large-scale synthesis - Method I. All polymerizations were performed according to the previously reported typical procedure (Table S7, entry 4−6).[26] Refer to the Supporting information for details.

All (co)polymers were recovered without purification as a brownish viscous liquid readily soluble in $CHCl_3$ and THF at 25 °C. All (co)polymer samples were stored under inert atmosphere at room temperature to avoid undesirable polycondensation of their alkoxysilyl groups with surrounding moisture, and analyzed rapidly following their preparation. The isolated α,ω-[(EtO)$_3$Si]$_2$-(PCOE)/PPG$^{(*)}$ (co)polymers were characterized by ^{1}H and 2D NMR and FTIR spectroscopies, and SEC analyses.

Preparation of films and tensile pieces from cured PCOE/PPG* SMPs synthesized from the two-step ROIMP/CM approach. The cured SMP materials were first shaped as tensile pieces that were cut out of thin films made from them. The following procedure was used to

obtain the films: 1) SMPs were put in an aluminum cup that was placed on a heating plate. When the sample was too viscous, the temperature was raised until complete softening of the polymer (ca. 30−65 °C). Then, the catalytic system (1wt% Neostan (S1) + 1wt% aminosilane promoter Geniosil (GF9) (Figure S28) was added and the mixture was manually stirred vigorously with a wooden spatula (thus being exposed to ambient moisture); 2) the mixture was then quickly poured on a silicone or polyethylene terephthalate (PET) foil (preheated when needed) and shaped into a 250 µm thin film by a film applicator; 3) the film was cured under controlled atmosphere (44% moisture, 25 °C) for 7 days (Figures S29−S31).

Tensile tests on the above-prepared tensile pieces. The thickness of the above-prepared tensile pieces was first measured to ensure their homogeneity; suitable values of 0.12–0.15 µm were thus obtained. A tensile piece was then placed in between two jaws, and the jaws then pulled the tensile piece (at a rate of 100 mm.min^{-1}) until its rupture. The strain applied as well as the elongation of the material at the rupture point were measured to give an indication of its strength and elasticity, respectively. Satisfactory standard deviations of 0.2 MPa for the strain-at-break, and 6−10% for the elongation at break were then obtained.

Results and discussion

Synthesis and characterization of PCOE/PPG$^{(*)}$-based SMPs by a ROIMP/CM approach.

The design of polyolefin/polyether based SMPs by metathesis reactions was focused on the tandem ROMP of a common cyclic olefin, COE, and insertion metathesis (IM) of commercially available polyethers such as tri(propyleneglycol) or poly(propyleneglycol$_{31}$diurethane) diacrylate (PPG$^{(*)}$), catalyzed by Grubbs' second generation catalyst (G2), associated with a CM using the bis(triethoxysilyl) diurethane CTA {(EtO)$_3$Si(CH$_2$)$_3$NHC(O)OCH$_2$CH=}$_2$ (CTA^{Et}) (Scheme 1). Indeed, G2 typically affords the best compromise in terms of price, commercial availability and efficiency. Also, the

13

diurethane CTA[Et] was previously shown to be highly effective in metathesis ROIMP reactions,[18–20,26] affording SMPOs with remarkable selectivities (typically less than 25wt% of cyclic nonfunctional poly(cyclooctene) (PCOE) side-product) and productivities (turnover number (TON) up to 95 000 $mol_{COE}.mol_{Ru}^{-1}$ and 5 000 $mol_{CTAEt}.mol_{Ru}^{-1}$).[18] Besides, CTA[Et] is straightforwardly prepared by the addition of 2-butene-1,4-diol to 3-(triethoxysilyl)propyl isocyanate in bulk conditions.[18] Also, CTA[Et] featuring acrylate functions cannot react with the alike PPG[(*)]'s acrylate functions,[35] thus implying that it can only be bound to a PCOE moiety, thereby driving the selectivity of the process and simplifying the characterization of the resulting polymers. The first screening experiments were performed using PPG, the one prepolymer providing simpler-to-analyze NMR spectra. Subsequent studies focused on the polyether diurethane PPG* segment, which is more valuable thanks to it readily availability and to its intrinsic urethane and aromatic moieties that may improve the properties of the ultimate materials.

The very first set of initial experiments, addressing either i) the CM of PPG or PPG* with several bis(trialkoxysilyl)alkene CTAs using various catalysts, or ii) the stepwise metathesis insertion of PPG into the already reported α,ω-bis(triethoxysilyl) PCOE (α,ω-[Si(OEt)$_3$]$_2$-PCOE)[17–20,26] in a ROMP/CM/IM approach, or iii) the ROIMP/CM of COE and PPG catalyzed by G2 in the presence of CTA[Et], all somehow featuring some limitation, are reported in the Supporting Information (Tables S2–S6; Schemes S3–S5; Figures S4–S14). Ultimately, polyolefin/polyether PPG*-based SMPs were successfully and effectively prepared by the one-pot, two-step ROIMP/CM strategy on a larger scale (Scheme 1, Method II), for the subsequent evaluation of their (post-curing) thermo-mechanical, rheological and adhesive properties, as described thereafter.

Synthesis of PCOE/PPG based SMPs by the one-pot, two-step ROIMP of COE and PPG and subsequent CM with CTA[Et] – Large-scale synthesis - Method II. The one-pot, two-

step procedure involving first the ROIMP of COE with PPG catalyzed by G2 ([COE]$_0$/[PPG]$_0$/[G2]$_0$ = 1500:500:1−10) under typical operating conditions (CH$_2$Cl$_2$, 40 °C, 2 h, argon flow; Table 1),[17−20] followed by the CM upon addition of CTA^{Et} (24 h; Table 2), successfully afforded the desired telechelic α,ω-bis(triethoxysilyl) PCOE/PPG alternated copolymers (Scheme 1).
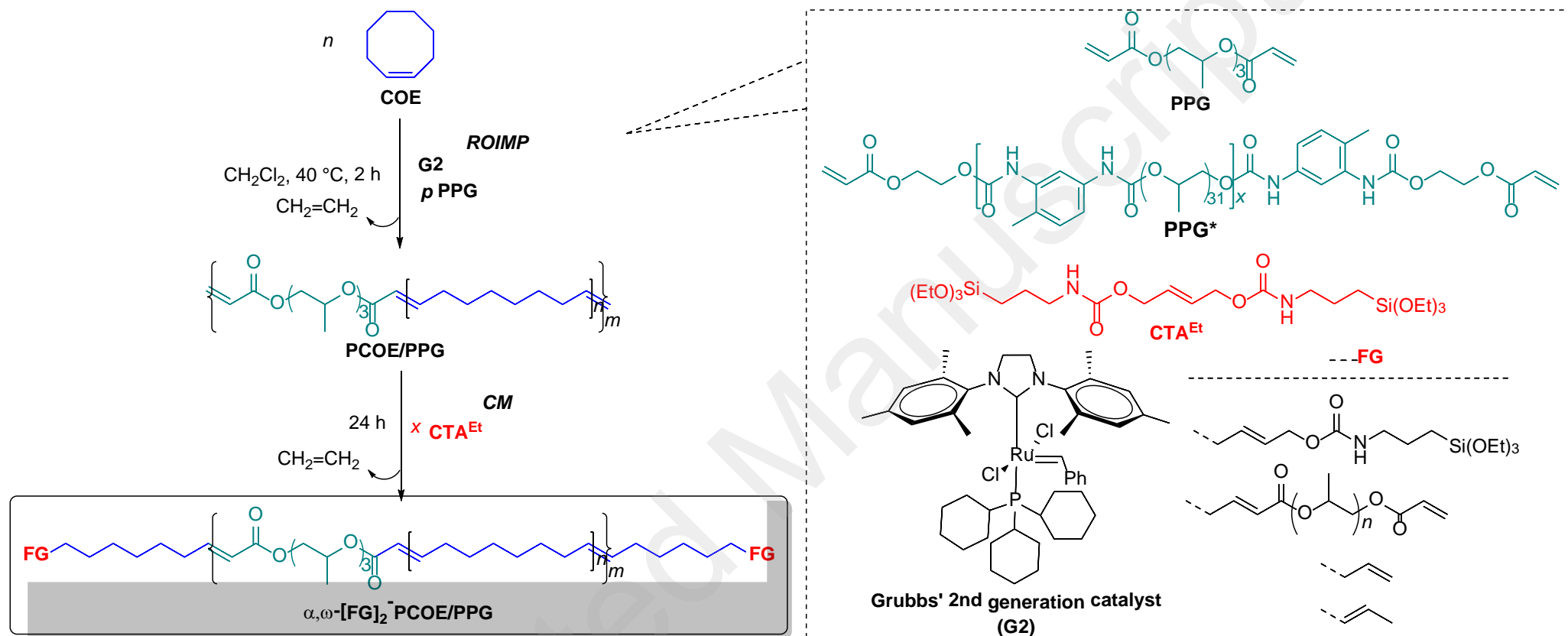
Scheme 1. Synthesis of α,ω-[Si(OEt)$_3$]$_2$-PCOE/PPG$^{(*)}$ by the one-pot, two step ROIMP of COE with PPG$^{(*)}$ and CM with CTA^{Et} catalyzed by

G2 – Method II, illustrated with PPG, and chemical structure of the poly(propyleneglycol) diacrylates (PPG$^{(*)}$), bis(triethoxysilyl) diurethane

CTA^{Et}, Grubbs' second generation catalyst G2, and of the possible chain-end groups (FG) of the (co)polymers investigated in the present work.

In the ROIMP first step, regardless of the addition mode of G2 catalyst (all at once or stepwise), a quasi-quantitative conversion of PPG's acrylate end-groups was reached. The high amount of ethylene released during the reaction (Scheme S7)[41] testified of the efficiency of the metathesis reactions, namely the ROIMP of COE/PPG and the CM between the C=C double bonds along the backbone and the acrylate moieties. The reaction was also highly effective, yet only when the catalyst was added stepwise in several aliquots, thus highlighting the importance to repeatedly introduce the catalyst by small portions over the course of the reaction rather than all at once. Under these operating conditions, the reproducibility was then excellent both in terms of acrylate conversion (99%) and ethylene released (89−94%)[41] (Table 1, entries 2−4; Scheme 1). On the other hand, isomerization of the terminal C=C double bond significantly increased with repeated additions and with larger contents of the catalyst (Vinyl/Isom. = 0.05 vs 11.3; Table 1, entry 1 vs entry 2). The difference observed between the molar mass values calculated ($M_{n,theo}$) and measured experimentally by SEC ($M_{n,SEC}$) most likely originates from the distinct hydrodynamic radii of PCOE/PPG copolymers and of polystyrene standards used for the calibration, and/or from the presence of cyclic polymers formed by ring-closing metathesis upon the release of ethylene.[17−20,41,42,43,44] NMR analyses (^{1}H, J-MOD, COSY, HSQC, HMBC; Figures S15−S18) of an aliquot of the crude ROIMP reaction mixture confirmed the presence of COE units ($H^{A−D}$, $C^{A−D}$), COE−PPG segments ($H^{E−I}$, $C^{E−I,M}$), along with residual acrylate ($H^{c,d}$, $C^{c,d}$), vinyl ($H^{a,b}$, $C^{a,b}$) and C=C isomerized (issued from the isomerization of vinyl groups; $H^{e−g}$, $C^{e−g}$) chain-end groups (Schemes 1,S6). Correspondingly, ESI-MS analysis of this same sample revealed the presence of linear non(alkoxysilyl) functional chains (i.e. terminated by a vinyl, an acrylate or an isomerized vinyl group; Figure S19, population in blue), and of cyclic nonfunctional chains (Figure S19, population in red) of alternated PCOE/PPG copolymers. These populations were also

observed with a missing or an additional CH_2 in the ring opened octene chain, evidencing the internal isomerization processes (Scheme S8).[17,18]

Table 1. ROIMP of COE and PPG catalyzed by G2 performed in CH_2Cl_2 at 40 °C during 2 h (Scheme 1) – Method II.

Entry	$[G2]_0$[a]	Conv._acrylate[b] (%)	Released ethylene[c] (%)	Polymer chain-end ratio[d]			$M_{n,theo}$[e] (g.mol^{-1})	$M_{n,SEC}$[f] (g.mol^{-1})	$Đ_M$[f]
				Acryl.	Vinyl	Isom.			
1	1/+1	77/98	83/90	14	79	7	6300	14 500	1.7
2	2/+2	90/99	70/89	2	5	92	6000	15 700	1.7
3	2/+2	90/99	43/89	2	5	94	6000	n.d.	n.d.
4	2/+2	96/99	72/94	5	30	65	7600	n.d.	n.d.
5	1+1/+2+2	95/99	72/91	9	0	91	6700	43 100	2.0
6	10	99	89	11	48	41	5600	n.d.	n.d.

[a] $[COE]_0/[PPG]_0 = 1500:500$, $[COE]_0+[PPG]_0 = 0.5$ M, reaction performed with under a flow of argon to remove the ethylene formed; reaction times were not optimized; 100 % conversion in COE as determined by ^1H NMR analysis (refer to the Experimental Section). [b] Conversion in PPG's acrylate functions as determined by ^1H NMR monitoring. [c] Determined by ^1H NMR spectroscopy; note that the amount of ethylene is underestimated.[41] [d] Ratio of acrylate (Acryl.), vinyl (Vinyl) and C=C isomerized (Isom.) chain end-groups as determined by ^1H NMR spectroscopy (refer to the Supporting Information; Scheme S6). [e] Theoretical molar mass calculated from the formula: $M_{n,theo} = \{([COE]_0 \times conv._{COE} \times M_{COE}) + ([PPG]_0 \times conv._{PPG} \times M_{PPG})\} / \{[PPG]_0 \times conv._{PPG} \times (1 - released\ ethylene)\}$ (refer to the Supporting Information), with $M_{COE} = 110$ g.mol^{-1} and $M_{PPG} = 300$ g.mol^{-1}. [f] Number-average molar mass ($M_{n,SEC}$) and dispersity ($Đ_M = M_w/M_n$) values determined by SEC vs polystyrene standards in THF at 30 °C. *n.d.* not determined.

Once complete conversion of the acrylate achieved, the second CM step was performed *in situ* (one-pot) upon the simultaneous addition to the reaction mixture of G2 and CTA^{Et} (Scheme 1). A single addition of two equiv of G2 revealed better than a stepwise addition in terms of CTA^{Et} conversion (86−97% vs ca. 75%, Table 2, entries 1−4, 6 vs 5). The amount of ethylene released[41] did not vary much from the ROIMP-step 1 to the CM-step 2, with a maximum increase of ca. 4% (within the uncertainty of the NMR measurements; Table 2).; this is most likely because most of the vinyl chains were consumed in the first ROIMP step and only a few isomerized, nonreactive ones remained. Under optimized conditions, a ratio of up to 66−73% of terminal ethoxysilyl end-functions was obtained, thus showing a fairly efficient CM reaction (Table 2, entries 1−5). As anticipated, $M_{n,SEC}$ values were systematically lower than the ones obtained after the first ROIMP step, due to the

18

redistribution of the chains mediated by the CTA during the CM ($M_{n,SEC\text{-}ROIMP}$ = 14 000−43 100 g.mol^{-1} vs $M_{n,SEC\text{-}ROIMP/CM}$ = 4400−6000 g.mol^{-1}; Table 1 vs Table 2 entries 1,2,5). The dispersity values of the copolymers ($Đ_M$ = 1.7−1.8) were typical of a metathesis process and similar to those reported from the ROIMP of cycloolefins with diacrylates (1.43−2.06).[33]

These results highlight that the ROIMP of COE and PPG first step is decisive: if high conversions in both acrylate and eventually released ethylene are reached, the targeted telechelic copolymer is likely to be formed from the following CM step, with a high molar mass and a high content of alkoxysilyl chain-end groups. In this regards, sequential addition of G2 in the first ROIMP step is thus compulsory (yet, at the expense of increasing isomerization), whereas the catalyst should be introduced at once in the last CM step.

NMR (^{1}H, J-MOD, COSY, HSQC, HMBC) and FT-IR analyses of the recovered telechelic α,ω-bis(triethoxysilyl) PCOE/PPG alternated copolymers (α,ω-[Si(OEt)$_3$]$_2$-PCOE/PPG), evidenced the same macromolecular structure as the one observed for PCOE/PPG copolymers obtained from the previous ROIMP step 1 (Figures S15−S18), along with the additional signals of the ethoxysilyl functional end-groups being clearly identified (H$^{a−i}$, C$^{a−i,q}$) (Figures 1,S20−S23). Furthermore, ESI-MS analysis provided another strong support for the formation of the telechelic alternated PCOE/PPG copolymers, including mono- and difunctional, linear non-functional, cyclic non-functional and internally isomerized polymers (Figure S24). Overall, these observations nicely demonstrated the formation of telechelic α,ω-bis(triethoxysilyl) PCOE/PPG alternated copolymers as major products with minor defects.

This latter tandem ROIMP/CM one-pot, two-step approach (Method II), along with the former simpler direct one-pot, one-step alike ROIMP/CM route (Method I, Refer to

Supporting Information),[26] thus provide two suitable synthetic pathways towards the targeted telechelic

α,ω-[(EtO)$_3$Si]$_2$-PCOE/PPG$^{(*)}$ alternated copolymers (Schemes 1,S5). These two strategies were then next implemented and optimized for the *larger scale* preparation of PCOE/PPG* SMPs to evaluate their thermo-mechanical and rheological properties before and after curing, and ultimately their adhesive ability.
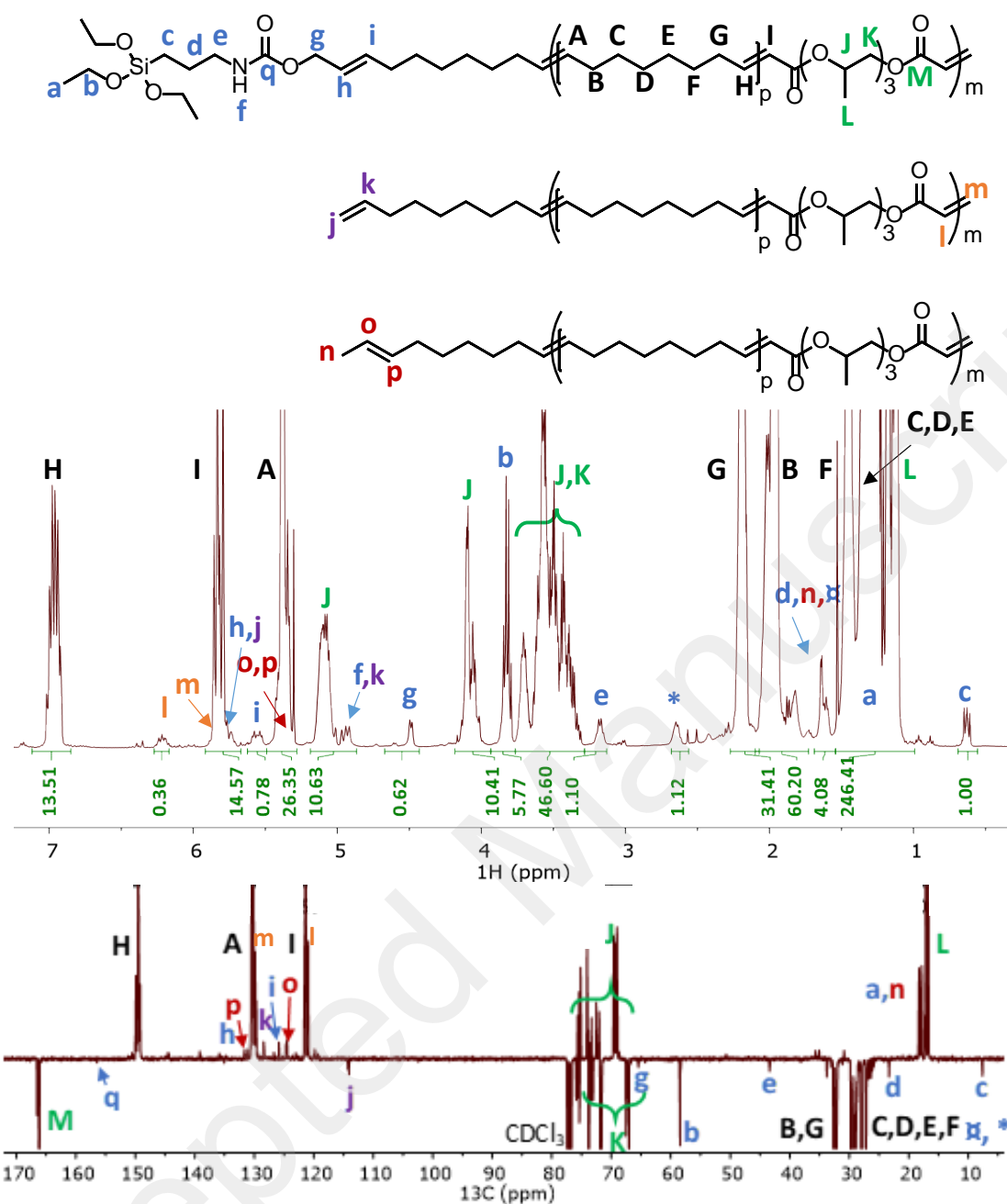
Figure 1. ^{1}H and J-MOD NMR spectra (400 and 100 MHz, 23 °C, CDCl$_3$) of an α,ω-[Si(OEt)$_3$]$_2$-PCOE/PPG sample isolated from the one-pot, two-step ROIMP/CM of COE and PPG catalyzed by G2 in the presence of CTA^{Et} (Scheme 1; Table 2, entry 6). Signals at δ$_{1H}$ 1.8 ppm and δ$_{13C}$ 35, 138 and 145 ppm could not be unambiguously assigned.

Table 2. CM of PCOE/PPG catalyzed by G2 in the presence of CTA^{Et} performed in CH_2Cl_2 at 40 °C during 24 h (Scheme 1) – Method II.[a]

Entry	PCOE/PPG (Table 1)	$[G2]_0$ (mol equiv)	$[CTA^{Et}]_0$ [b] (mol equiv)	$Conv._{CTAEt}$ [b] (%)	Released ethylene[b] (%)	Polymer chain-end ratio[b]				$M_{n,theo}$ [c] (g.mol^{-1})	$M_{n,SEC}$ [d] (g.mol^{-1})	$Đ_M$ [d]
						Acryl.	Si(OEt)$_3$	Vinyl	Isom.			
1	Entry 1	2	100	88	90	1	70	20	9	2600	6000	1.7
2	Entry 2	2	100	86	91	3	67	0	30	3000	4900	1.7
3	Entry 3	2	100	87	93	3	73	0	24	3300	4900	1.8
4	Entry 4	2	100	97	94	3	66	4	27	2700	5000	1.7
5	Entry 5	1/+1	100	72/74	87/94	3	72	0	25	3600	4400	1.7
6	Entry 6	1	20	90	91	8	23	22	47	2900	6500	1.7

[a] Reaction performed under a flow of argon to remove the ethylene formed; $[COE]_0+[PPG]_0 = 0.5$ M, $[G2]_0 = 0.2$ mol%; 100 % conversion in COE as determined by ^{1}H NMR analysis (refer to the Experimental Section). [b] Determined by ^{1}H NMR spectroscopy (refer to the Experimental Section). [c] Calculated from the formula: $M_{n,theo} = ([COE]_0 \times conv._{COE} \times M_{COE} + [PPG]_0 \times conv._{PPG} \times M_{PPG} + [CTA^{Et}]_0 \times conv._{CTAEt} \times M_{CTAEt})$ / $([PPG]_0 \times conv._{PPG} \times (1 - release_{ethylene}) + [CTA^{Et}]_0 \times conv._{CTAEt})$, with $M_{COE} = 110$ g.mol^{-1}, $M_{PPG} = 300$ g.mol^{-1} and $M_{CTAEt} = 582$ g.mol^{-1}. [d] Number-average molar mass ($M_{n,SEC}$) and dispersity ($Đ_M = M_w/M_n$) values determined by SEC vs polystyrene standards in THF at 30 °C.

22

Thermal, rheological, mechanical and adhesive properties of (cured) α,ω-[(EtO)₃Si]₂-PCOE/PPG* SMPs.

1. Thermal and rheological properties of α,ω-[(EtO)₃Si]₂-PCOE/PPG* SMPs before curing.

The thermal and rheological properties of PCOE/PPG* SMPs, referred to as PCOE^x/PPG*^{y}-CTA^{Etz} copolymers (with x, y, z = weight fraction of PCOE, PPG*, and CTA^{Et} and x + y + z = 100 wt%; $M_{n,SEC}$ ca. 13 000 g mol^{-1}, $Đ_M$ ca 2.3), prepared from the two-step ROIMP/CM approach – large-scale synthesis Method II (ca. 100 g; refer to the Experimental Section; Scheme 1), have been studied before curing. They were then compared to the alike previously reported copolymers synthesized from the one-step ROIMP/CM Method I (Scheme S5), as previously characterized[26] (Table S7; Figure S25). A Si(OEt₃)₂ weight fraction of z = 0.15 was essentially considered in the present work since our previous investigations showed that a higher trialkoxysilyl content (z = 0.22) disfavored the copolymer thermal stability, while not significantly modifying its thermal transition temperatures (Table 3).[26] The SMPs performances were benchmarked against a commercially available triethoxysilyl-functionalized polybutadiene used as adhesives resin (Polyvest E100). Polyvest E100 was selected, among the very few alkoxysilane-terminated polybutadiene available on the commercial market, for its low viscosity, a characteristic required for adhesive applications. Due to its unsaturated backbone and terminal Si(OEt)₃ functionalities, this apolar and hydrophobic resin is used as a highly reactive binder for its very good dispersing properties of inorganic fillers in various fields of applications (in particular as adhesives and sealants, or as additive for tires, waterproofing membranes and coatings, dispersion additive for rubber based formulations).[45]

TGA analyses of PCOE/PPG*-CTA^{Et15} SMPs (Method II) of similar molar mass ($M_{n,SEC}$ ca. 13 000 g mol^{-1}, $Đ_M$ = 2.5) showed that inclusion of more temperature sensitive

PPG* segments along the polyolefin, greatly and proportionally alters its thermal stability ($T_d^{10\%}$ = 406 vs 258–275 °C; Table 3, entry 2 vs 3–5; Table S8). All the PCOE/PPG*-CTA^{Et15} copolymers displayed a three-step degradation profile, corresponding to first the polycondensation and degradation of triethoxysilyl functions (ca. 150–250 °C), followed by the degradation of the PPG* segments (ca. 250–350 °C), and then the degradation of PCOE units (ca. 350–450 °C) (Figure S26). The thermal degradation profile of the samples prepared in the present work from the two-step ROIMP/CM Method II (Scheme 1) is the same as the one observed for the alike PCOE/PPG* samples obtained from the similar one-step ROIMP/CM Method I (Scheme S5).[26] The copolymers prepared from the two-step tandem ROIMP/CM Method II exhibited a slightly lower stability (ΔT_d ca. 20–33 °C) than the previously reported samples prepared from the direct route Method I (Table S8);[26] this is possibly due to the presence of residual PPG* oligomers within PCOE^{35}/PPG*^{50}-CTA^{Et15} reported herein that may act as plasticizers (*vide supra*, Figure S25). DSC analysis of all PCOE^x/PPG*^{y}-CTA^{15} copolymers showed a semi-crystallinity that slightly increases with higher PCOE contents (Table 3, Figure S26).[46] The comparison with a PPG*-free PCOE-CTA^{Et} sample (Table 3, entry 2)[18] highlights the significant increase in glass transition temperature values for the PCOE/PPG*-CTA^{Et15} SMPs (ΔT_g ca. 18 °C), while upon PPG* inclusion, the crystallization (T_c) and the melting (T_m) temperatures were recorded at lower values and the crystallinity decreased drastically (ΔH_{cryst} ca. −103 J.g^{-1}). Copolymers obtained from the one-step ROIMP/CM Method I that we previously reported[26] generally displayed higher T_g and crystallinity than those prepared herein from the two-step Method II; this possibly originates from an earlier polycondensation during the DSC analysis that generates siloxane bridges which improve the thermal stability, as corroborated by TGA measurements. On the other hand, the benchmarked Polyvest E100 (of yet a lower molar mass) was shown to

be amorphous and more thermally stable ($T_d^{10\%}$ = 329 °C) than any of the uncured PCOE/PPG*-CTA^{Et15} SMPs, regardless of their synthetic route (Table 3, Figure S26).[26]

Table 3. TGA and DSC thermal characteristics of α,ω-[(EtO)$_3$Si]$_2$-PCOE/PPG* synthesized by the one-pot, two-step ROIMP/CM route – large-scale synthesis (Method II), before and after curing (Table S7).

Entry	Polymer	Before curing		After curing		Before curing				After curing			
		$T_d^{10\%[a]}$ (°C)	$T_d^{20\%[a]}$ (°C)	$T_d^{10\%[a]}$ (°C)	$T_d^{20\%[a]}$ (°C)	$T_g^{[b]}$ (°C)	$T_c^{[b]}$ (°C)	$T_m^{[b]}$ (°C)	$\Delta H_{cryst}^{[b]}$ (J.g^{-1})	$T_g^{[b]}$ (°C)	$T_c^{[b]}$ (°C)	$T_m^{[b]}$ (°C)	$\Delta H_{cryst}^{[b]}$ (J.g^{-1})
1	PPG*	294	317	-	-	−45	-	-	-	-	-	-	-
2 [18]	α,ω-[Si(OEt)$_3$]$_2$-PCOE	406	425	*n.d.*	*n.d.*	−78	40	56	−111	*n.d.*	*n.d.*	*n.d.*	*n.d.*
3	PCOE^{20}/PPG*^{65}-CTA^{Et15}	258	294	314	382	−61	6	52	−4	−63	−9	47	−4
4	PCOE^{35}/PPG*^{50}-CTA^{Et15}	275	338	299	370	−56	23	41	−6	−63	8	54	−11
5	PCOE^{50}/PPG*^{35}-CTA^{Et15}	266	339	284	353	−62	30	43	−13	*n.o.*	17	54	−23
6	Polyvest E100 [c]	329	424	388	427	−50	-	-	-	*n.o.*	-	-	-

[a] Degradation temperatures determined by TGA with T_d^x = temperature at which x% of mass loss occurs (refer to Supporting Information).
[b] Glass transition (T_g), crystallization (T_c) and melting (T_m) temperatures, and crystallization enthalpy (ΔH_{cryst}) determined by DSC (refer to the Supporting Information). [c] $M_{n,SEC}$ = 5700 g.mol^{-1}, refer to the Experimental Section. *n.d.* not determined; *n.o.* not observed.

26

The viscosities of α,ω-[Si(OEt)₃]₂-PCOE/PPG* prepared herein from the two-step ROIMP/CM Method II feature a rheofluidifying behavior below their T_m (i.e. at 30 °C). A quite high viscosity at low share rate ($\eta^{\gamma=0.1}$ = 3000−11 000 Pa.s) and a low viscosity at high share rate ($\eta^{\gamma=100}$ = 21−270 Pa.s) were recorded, while the viscosity generally increases with higher molar mass copolymers. Above their T_m (i.e. at 60 °C), the copolymers then display a Newtonian behavior along with a lower viscosity ($\eta^{\gamma=0.1}$ = 4−12 Pa.s, $\eta^{\gamma=100}$ = 3−8) (Table 4; Figure 2). A similar rheological behavior was observed with the alike previously reported copolymers prepared from the direct one-step approach Method I (Table S9);[26] on the other hand, Polyvest E100 displays a Newtonian behavior at 30 °C (Table 4; Figure 2).

All these SMPs combine a rather high thermal stability and low crystallinity, with a very low viscosity either under stress or temperature, thereby foreseeing easy processing and hinting at promising industrial outcomes.

Table 4. Rheological characteristics of α,ω-[(EtO)₃Si]₂-PCOE/PPG* SMPs synthesized by the one-pot, two-step ROIMP/CM route – large-scale synthesis (Method II) (Table S7, S10).

Entry	SMP	T = 30 °C [a]			T = 60 °C [a]		
		$\eta^{\gamma=0.1}$ (Pa.s)	$\eta^{\gamma=100}$ (Pa.s)	Rheological behavior	$\eta^{\gamma=0.1}$ (Pa.s)	$\eta^{\gamma=100}$ (Pa.s)	Rheological behavior
1	PPG*	58	33	Rheofluidifying	-	-	-
2 [18]	α,ω-[Si(OEt)₃]₂-PCOE	n.d.[b]	n.d.[b]	n.d.[b]	n.d.[b]	n.d.[b]	n.d.[b]
3	PCOE²⁰/PPG*⁶⁵-CTA^Et15	11 000	270	Rheofluidifying	12	8	Newtonian
4	PCOE³⁵/PPG*⁵⁰-CTA^Et15	6300	130	Rheofluidifying	3	3	Newtonian
5	PCOE⁵⁰/PPG*³⁵-CTA^Et15	6700	21	Rheofluidifying	4	3	Newtonian
6	Polyvest E100	8	7	Newtonian	-	-	-

[a] Viscosity and rheological behavior as determined by viscosimetry using a Contraves Low Shear 30 viscosimeter; uncertainty = ±5% (refer to Supporting Information). [b] *n.d.* Not determined because the polymer is solid.
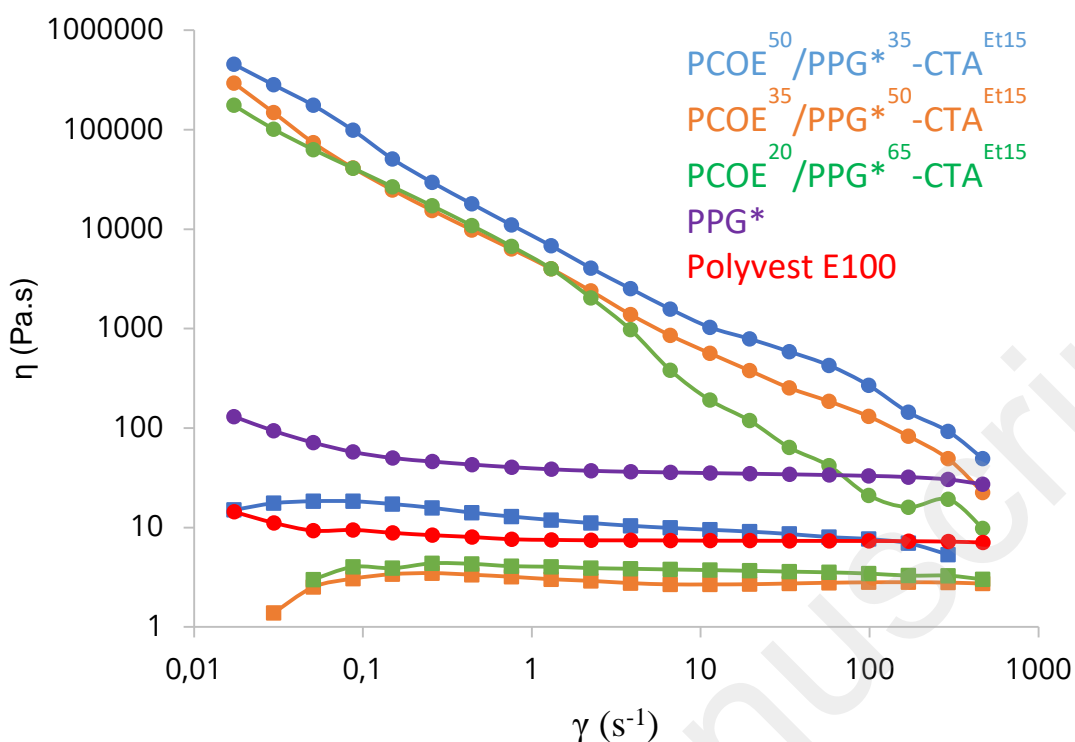
27

Figure 2. Viscosity as a function of shear rate measured at 30 °C (dots) and 60 °C (squares) for α,ω-[(EtO)$_3$Si]$_2$-PCOE/PPG* SMPs synthesized by the two-step ROIMP/CM route – Method II (Table 4, S10). The last two data points depicted in the curves have most likely been impacted by the mass loss occurring during the rotation at high shearing and should thus not be taken into account.

2. Thermo-mechanical properties of α,ω-[(EtO)$_3$Si]$_2$-PCOE/PPG* SMPs after curing.

The α,ω-[(EtO)$_3$Si]$_2$-PCOE/PPG* copolymers synthesized from the two-step ROIMP/CM – large-scale synthesis Method II, were then cured using the previously successfully investigated catalytic system composed of the organotin(IV) catalyst Neostan (S1, 1wt%) and aminosilane promoter Geniosil (GF9, 1wt%), and surrounding moisture (Figure S28).[4,26,47,48] Homogenous and solid films obtained from the cured PCOE/PPG* SMPs samples, then provided tensile pieces suitable for thermo-mechanical investigations (Figures S29–S31). Note that following this same procedure, cross-linked (COE-free) α,ω-[Si(OEt)$_3$]$_2$-PPG*

generated a film that was too fragile to afford cohesive-enough tensile pieces. Also, the previously reported α,ω-[(EtO)$_3$Si]$_2$-PCOE/PPG* copolymers prepared from the direct/one-step ROIMP/CM Method I,[26] turned out to be too hard to be stretched into an homogeneous film; this prevented the elaboration of suitable tensile pieces and precluded comparison of their thermo-mechanical properties to those of the copolymers herein investigated.

As expected, the formation of a siloxane network upon curing clearly increased the thermal stability of the SMPs, as revealed by TGA analysis (Table 3; following curing: $\Delta T_d^{10\%}$ ca. +33, $\Delta T_d^{20\%}$ ca. +44 °C). In particular, the thermograms evidenced the disappearance of the first degradation step, while the second one remained unchanged (Figure S26). In addition, all thermal transition temperatures, except the melting temperature, significantly decreased upon curing ($\Delta T_c = -(2-7)$ °C; $\Delta T_g = -(13-15)$ °C; $\Delta T_m = +12$ °C). Also, the cross-linked SMPs were more crystalline (Table 3; before curing ΔH_{cryst} ca. -8.5 J.g^{-1}, after curing, ΔH_{cryst} ca. -13.5 J.g^{-1}). These thermal profiles are yet difficult to be further rationalized in light of the complex structure of these materials and given the limited literature reports on the thermal stability of SMPs.

The viscoelastic behavior of the SMP materials reported herein has been investigated by DMA (Figure 3; Table S11). Polyvest E100 film displayed a rather constant modulus and only one rubbery plateau with a relatively high E' modulus. The peak at ca. 100 °C on the tan δ = E''/E' originates from both the increase of the loss modulus (E'') and the drop of the storage modulus (E'). This tan δ peak indicated a high mobility of the polymer in the 3D network, the latter which yet did not enable the material to flow (the two E'' and E' curves staying separated, i.e. not crossing each other). For α,ω-[(EtO)$_3$Si]$_2$-PCOE/PPG* copolymers cured with S1/GF9 (1:1wt%), a first plateau appeared at ca. 25 °C (Figure 3b,d, Table S11) with the corresponding E' value increasing with the PCOE content (Table S11, entries 2−4);

this highlighted the cohesion and mechanical strength imparted by PCOE units. After the first rubbery plateau, the elastic contribution *E'* dropped again. This second plateau was indicative of the PCOE melting: the larger the PCOE content, the larger the drop (Table S11, entries 2−4). We assumed that the first plateau was much higher due to the various contributions of entanglements of amorphous parts, of crystalline areas and of cross-linked chains. Thus, when the crystalline moieties merge, part of the rigid network is lost and the *E'* modulus falls down. Finally, these PCOE/PPG* cross-linked copolymers do not display the second peak of tan *δ* observed with Polyvest E100. Instead, *E'* and *E''* remain more constant, representative of a stiffer 3D network.
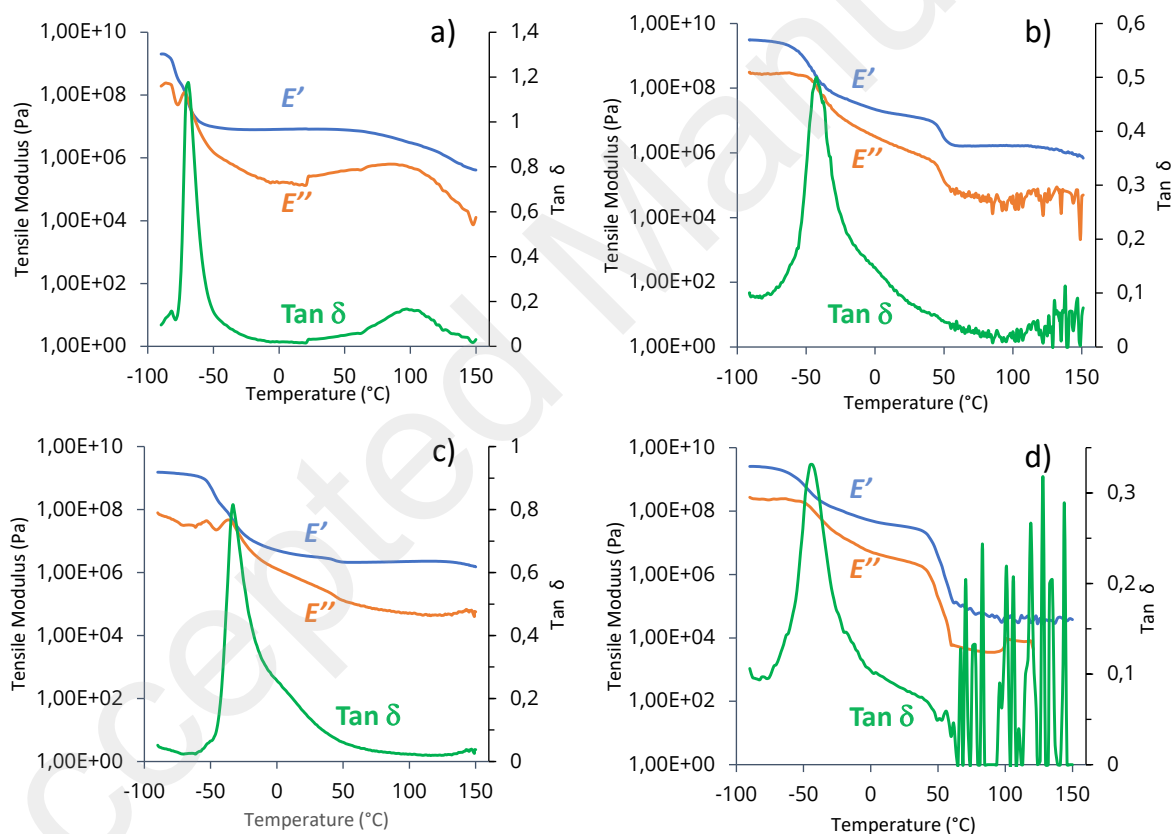

Figure 3. *E'*, *E''* and Tan *δ* as a function of temperature measured by DMA analysis of a) Polyvest E100, and of b–d) S1/GF9 (1:1wt%)-cured α,ω-[(EtO)$_3$Si]$_2$-PCOE/PPG* SMPs synthesized by the one-pot, two-step ROIMP/CM route (Method II), namely b)

PCOE^{20}/PPG*^{65}-CTA^{Et15}, c) PCOE^{35}/PPG*^{50}-CTA^{Et15}, and d) PCOE^{50}/PPG*^{35}-CTA^{Et15} (Table S11).

The average entanglement molecular weight (M_e) within the 3D networks has been estimated through a model based on the elastic deformation using the formula M_e (g.mol^{-1}) = ($\rho \times$ R $\times$ T)/E', where ρ is the density of the material, R the ideal gas constant, T the temperature and E' = the storage modulus at this temperature (Table 5).[49] However, since the present SMPs feature distinct segments, calculated M_e values will deviate from the initial calculation model and will only be indicative of the 3D network. Also, Polyvest E100 (M_e = 300 g.mol^{-1}; Table 5, entry 1) cannot reliably be compared to the SMPs due to their molecular differences. Since a larger PCOE content improved the chain flexibility, it induced more entanglements and thus lowered the corresponding M_e value, as experimentally observed on the first plateau (Table 5, entries 2−4). M_e evolution at the second plateau basically followed the trend observed at the first plateau, except for the PCOE^{35}/PPG*^{50}-CTA^{Et15} cross-linked copolymer for which M_e values were lower than expected (Table 5, entries 3). The differences observed between values at the two plateaus may arise from the difficulty to maintain a constant tension on the film after the second transition, due to the softening and relaxing of the film, thereby inducing some imprecision on the measurements.

Table 5. Calculated Me values of S1/GF9(1:1wt%)-cured α,ω-[(EtO)$_3$Si]$_2$-PCOE/PPG* SMPs synthesized by the one-pot, two-step ROIMP/CM route – large-scale synthesis (Method II).

Entry	SMPs	ρ (kg.m$^{-3)}$	T (°K)	E' (MPa)		M_e (g.mol^{-1})	
				1st rubbery plateau	2nd rubbery plateau	1st rubbery plateau	2nd rubbery plateau
1	Polyvest E100	997	298	8.4	-	300	-
2	PCOE^{20}/PPG*^{65}-CTA^{Et15}	892	298	3.2	1.6	700	1850
3	PCOE^{35}/PPG*^{50}-CTA^{Et15}	1014	298	13.7	8.7	250	3500
4	PCOE^{50}/PPG*^{35}-CTA^{Et15}	957	289	32.8	22.0	80	1350

The mechanical properties of the S1/GF9(1:1wt%)-cured α,ω-[(EtO)$_3$Si]$_2$-PCOE/PPG* SMPs prepared from the two-step ROIMP/CM route – large-scale synthesis (Method II) were evaluated from tensile tests using the tensile pieces cut out from the films (refer to the Experimental Section). PCOE units were shown to provide strength and rigidity to the cross-linked copolymer materials, whereas PPG* units imparted elasticity, thereby confirming DMA data. All PCOE/PPG* SMPs reported herein showed a higher elongation-at-break than Polyvest E100, the benchmark material with a sole polyolefin backbone (Figure 4a). The cured PCOE^{50}/PPG*^{35}-CTA^{Et15} afforded the best compromise with the highest strain-at-break (3.3 MPa) and a good elongation-at-break (44%), both being superior to those of Polyvest E100 (2.2 MPa and 40%, respectively). This is actually not surprising as PCOE^{50}/PPG*^{35}-CTA^{Et15} SMP also displayed the lowest M_e values (80 and 1350 g.mol^{-1}; Table 5, entry 4), highlighting a denser and stiffer network. These results thus foresee PCOE/PPG-CTA^{Et} copolymers as materials with promising mechanical properties for CASE applications.
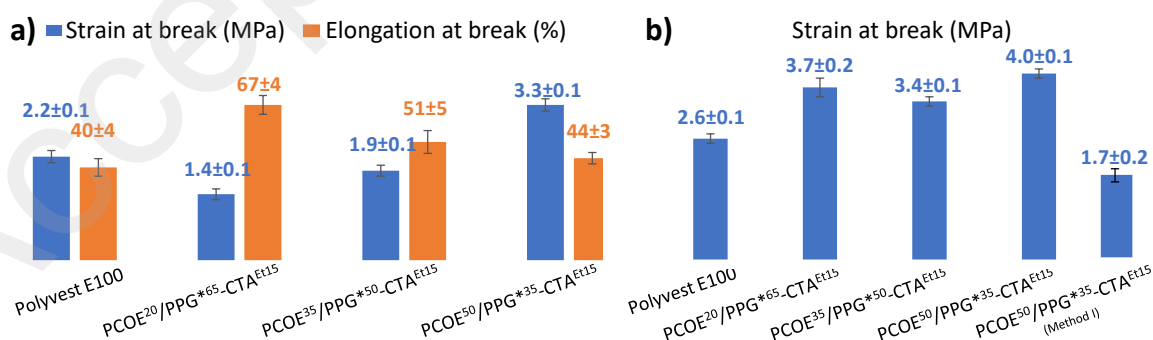

Figure 4. a) Strain-at-break (■) and elongation-at-break (■) of S1/GF9(1:1wt%)-cured α,ω-[(EtO)$_3$Si]$_2$-PCOE/PPG* SMPs synthesized by the one-pot, two-step ROIMP/CM route – large-scale synthesis (Method II). The results are representative of at least four experiments

performed on each cross-linked alternated copolymer sample; b) Strain-at-break of adhesives on wood made from S1/GF9(1:1wt%)-cured α,ω-[(EtO)$_3$Si]$_2$-PCOE/PPG* SMPs prepared from the one-pot, two-step ROIMP/CM route (large-scale synthesis, Method II − middle three ones −, and previously reported Method I − far right −[26]), and benchmarked with Polyvest E100 −far left.

3. Adhesion efficiency of cured α,ω-[(EtO)$_3$Si]$_2$-PCOE/PPG* SMPs.

The adhesion efficiency of the S1/GF9(1:1wt%)-cured α,ω-[(EtO)$_3$Si]$_2$-PCOE/PPG* SMPs synthesized by the two-step ROIMP/CM route – large-scale synthesis (Method II) was then evaluated and benchmarked against Polyvest E100 (Figure 4b). All PCOE/PPG* cross-linked SMPs showed good adhesion, with a strain-at-break of 3.4(0.1)−4.0(0.1) MPa, significantly superior to that of Polyvest E100 (strain-at-break value of 2.6(0.1) MPa). We assume that PPG* imparted a better elasticity to the polyolefin segment, in agreement with the above-mentioned DMA and tensile data. Surprisingly enough, the PCOE/PPG* ratio did not seem to really impact the adhesive properties. In comparison, the previously reported S1/GF9(1:1wt%)-cured PCOE^{50}/PPG*^{35}-CTA^{Et15} SMPs synthesized by the one-step ROIMP/CM Method I,[26] displayed a twice as low strain-at-break as the alike copolymer prepared in the present work by the two-step route – large-scale synthesis (Method II) (1.7[26] vs 4.0 MPa, respectively). This most likely originates from the presence, within the present copolymer sample, of larger amounts of plasticizing oligomers (as evidenced by SEC analyses, Figure S25) that provide a higher resistance to strain.

Conclusion

Several original bis(trialkoxy)-functional polyether/polyolefin alternated copolymer materials were synthesized by Ru-catalyzed metathesis reactions following distinct CM, ROIMP/CM,

or ROMP/CM/IM strategies. Among these latter approaches, the herein described one-pot, two-step tandem ROIMP of COE with PPG* and subsequent CM with CTA^{Et} (Method II, Scheme 1) revealed most performant for the large scale preparation of the desired SMPs. α,ω-[Si(OEt)$_3$]$_2$-PCOE/PPG* materials featuring various ether-to-olefins ratios were then prepared ($M_{n,SEC}$ up to 14 000 g.mol^{-1}) and characterized molecularly by NMR and SEC investigations. The polyether/polyolefin copolymers showed lower thermal stability and thermal characteristics (T_m and T_c) than both a PCOE (PPG*-free homopolymer) or the benchmark polybutadiene Polyvest E100 (Tables 3,S7). Oligomers present alongside the desired copolymers (as evidenced by SEC analyses; Figure S25) acted as plasticizers, enhancing in turn the thermal, mechanical and adhesive properties of the materials, as well as their ease of processability. The alternated copolymer samples were isolated as rheofluidifying solids, *i.e.* materials that behave as a solid under a weak solicitation, yet as a fluid when a force is applied onto them.

After curing of these SMPs from moisture using the catalyst system S1/GF9, DMA measurements evidenced that PPG* segments enhanced the elasticity of the cross-linked materials as compared to Polyvest E100 (Figure 3). Strains-at-break recorded from tensile tests were generally similar to that of Polyvest E100, while wood adhesion properties revealed superior for the PCOE/PPG* copolymers (Figure 4). Comparison of materials with different PCOE-to-PPG* ratio suggested that the higher the content in PCOE in the cross-linked alternated copolymers, the higher the thermal stability, the crystallinity, and the strength of the SMPs; however, the elasticity and the cross-linking density determined by DMA were then lower (Figure 3; Tables 3,5,S11). These cured PCOE/PPG* SMP materials showed a better resistance to strain than the previously reported alike PCOE/PPG* materials prepared from a direct one-step procedure (Method I).[26]

The herein exploited ROIMP/CM strategy towards the large-scale preparation of alternated polyether/polyolefin (Method II) successfully provides monocomponent SMPs with promising thermal, mechanical and especially, adhesives characteristics (strain-at-break on wood up to 4.0 MPa) improved as compared to the benchmarked industrial Bostik adhesive Polyvest E100. Envisioned outcomes of these polyether/polyolefin materials are in particular for CASE applications requiring improved resistance to humidity and hydrolysis (as imparted by the polyolefin segments), and for (semi)structural bonding applications in automotive or transport markets. These preliminary results, obtained without optimization nor formulation of the adhesives (*i.e.* free of any additives, fillers or charges), can likely be further improved to enhance their properties and widen the field of applications, in particular as viable alternative to current polyurethane adhesives.[50]

ASSOCIATED CONTENT

Supporting Information

The Supporting Information including detailed and complementary experimental section and complementary data on the PCOE/PPG* copolymers, is available free of charge on the ACS Publications website at DOI: XXX/.

AUTHOR INFORMATION

Corresponding Author

*E-mail: jean-francois.carpentier@univ-rennes1.fr; sophie.guillaume@univ-rennes1.fr

ORCID

Jean-François Carpentier: 0000-0002-9160-7662, Sophie M. Guillaume: 0000-0003-2917-8657

NOTES

The authors declare no competing financial interest.

ACKNOWLEDGEMENTS

References

1 Da Silva, L. F. M.; Öchsner, A.; Adams, R. D. *Handbook of Adhesion Technology*, Springer, 2011.

2 Ebnesajjad, S. *Handbook of Adhesives and Surface Preparation*, Elsevier Inc., 2011.

3 Mittal, K. L.; Pizzi, A. *Handbook of Sealant Technology*, CRC Press: Boca Raton (FL), 2009.

4 Pizzi, A.; Mittal, K. L. *Handbook of Adhesive Technology*, CRC Press, Taylor & Francis Group, 2017.

5 Chruściel, J. J.; Leśniak, E. *Modification of Thermoplastics with Reactive Silanes and Siloxanes*, in Thermoplastic Elastomers, Adel El-Sonbati Ed., InTech, 2012, Chap 9, p 155–192.

6 Owen, M. J.; Dvornic P. R. *Advances in Silicon Science*, Vol. 4, Springer, 2012.

7 Lee L. H. in *Adhesion Science and Technology*, Plenum Press, New York, 1975.

8 Ceresana, *Market Study: Adhesives - World (3rd Edition)*, **2017**.

9 A. Kinloch, *Adhesion and Adhesives Science and Technology*, **1987**.

10 Guillaume, S. M. Advances in the synthesis of silyl-modified polymers (SMPs). *Polym. Chem.* **2018**, 1911–1926.

11 Chung, T. C.; Chasmawala, M. Synthesis of telechelic 1,4-polybutadiene by metathesis reactions and borane monomers. *Macromolecules* **1992**, *25*, 5137–5144.

12 Hillmyer, M. A.; Grubbs, R. H. Preparation of hydroxytelechelic poly(butadiene) via ring-opening metathesis polymerization employing a well-defined metathesis catalyst. *Macromolecules* **1993**, *26*, 872–874.

13 Hillmyer, M. A.; Grubbs, R. H. Chain Transfer in the Ring-Opening Metathesis Polymerization of Cyclooctadiene Using Discrete Metal Alkylidenes. *Macromolecules* **1995**, *28*, 8662–8667.

14 Pitet, L. M.; Hillmyer, M. Carboxy-Telechelic Polyolefins by ROMP Using Maleic Acid as a Chain Transfer Agent. *Macromolecules* **2011**, *44*, 2378–2381.

15 Bielawski, C. W.; Benitez, D.; Morita, T.; Grubbs, R. H. Synthesis of End-Functionalized Poly(norbornene)s via Ring-Opening Metathesis Polymerization. *Macromolecules*, **2001**, *34*, 8610-8618.

[16] Morita, T.; Maughon, B. R.; Bielawski, C. W.; Grubbs, R. H. A Ring-Opening Metathesis Polymerization (ROMP) Approach to Carboxyl- and Amino-Terminated Telechelic Poly(butadiene)s. *Macromolecules* **2000**, *33*, 6621–6623.

[17] Diallo, A. K.; Michel, X.; Fouquay, S.; Michaud, G.; Simon, F.; Brusson, J.-M.; Carpentier, J.-F.; Guillaume, S. M. α-Trialkoxysilyl Functionalized Polycyclooctenes Synthesized by Chain-Transfer Ring-Opening Metathesis Polymerization. *Macromolecules* **2015**, *48*, 7453–7465.

[18] Michel, X.; Fouquay, S.; Michaud, G.; Simon, F.; Brusson, J.-M.; Carpentier, J.-F.; Guillaume, S. M. α,ω-Bis(Trialkoxysilyl) Difunctionalized Polycyclooctenes from Ruthenium-Catalyzed Chain-Transfer Ring-Opening Metathesis Polymerization. *Polym. Chem.* **2016**, *7*, 4810–4823.

[19] Michel, X.; Fouquay, S.; Michaud, G.; Simon, F.; Brusson, J.-M.; Carpentier, J.-F.; Guillaume, S. M. Simple Access to Alkoxysilyl Telechelic Polyolefins from Ruthenium-Catalyzed Cross-Metathesis Depolymerization of Polydienes. *Eur. Polym. J.* **2017**, *96*, 403–413.

[20] Michel, X.; Fouquay, S.; Michaud, G.; Simon, F.; Brusson, J.-M.; Roquefort, P.; Aubry, T.; Carpentier, J.-F.; Guillaume, S. M. Tuning the Properties of α,ω-Bis(Trialkoxysilyl) Telechelic Copolyolefins from Ruthenium-Catalyzed Chain-Transfer Ring-Opening Metathesis Polymerization (ROMP). *Polym. Chem.* **2017**, *8*, 1177–1187.

[21] Yuan, Y.; Zhang, Y.; Fu, X.; Kong, W.; Liu, Z.; Hu, K.; Jiang, L.; Lei, J. Molecular design for silane-terminated polyurethane applied to moisture-curable pressure-sensitive adhesive. *J. Appl. Polym. Sci* **2017**, *134*, 45292.

[22] Matloka, P. P.; Kean, Z.; Wagener, K. B. Chain Internal/Chain End Latent Crosslinking in Thermoset Polymer Systems. *J. Polym. Sci. Part A* **2010**, *48*, 1866–1877.

[23] Matloka, P. P.; Kean, Z.; Greenfield, M.; Wagener, K. B. Synthesis and Characterization of Oligo(Oxyethylene)/Carbosilane Copolymers for Thermoset Elastomers via ADMET. *J. Polym. Sci. Part A* **2008**, *46*, 3992–4011.

[24] Jiang, H.; Zheng, Z.; Song, W.; Li, Z.; Wang, X. Alkoxysilane Functionalized Polyurethane/Polysiloxane Copolymers: Synthesis and the Effect of End-Capping Agent. *Polym. Bull.* **2007**, *59*, 53–63.

[25] Matloka, P. P.; Sworen, J. C.; Zuluaga, F.; Wagener, K. B. Chain-End and Chain-Internal Crosslinking in Latent Reactive Silicon Elastomers. *Macromol. Chem. Phys.* **2005**, *206* (2), 218–226.

26 Chauveau, C.; Fouquay, S.; Michaud, G.; Simon, F.; Carpentier J.-F.; and Guillaume, S. M. α,ω-Bis(trialkoxysilyl) Telechelic Polyolefin/Polyether Copolymers for Adhesive Applications Using Ring-Opening Insertion Metathesis Polymerization Combined with a Chain-Transfer Agent. *ACS Appl. Polym. Mater.,* **2019**, *1*, 1540–1546.

27 Ilker, M. F.; Coughlin, E. B. Alternating Copolymerizations of Polar and Nonpolar Cyclic Olefins by Ring-Opening Metathesis Polymerization. *Macromolecules* **2002**, *35*, 54–58.

28 Amir-Ebrahimi, V.; Rooney, J. J. Remarkable alternating effect in metathesis copolymerization of norbornene and cyclopentene using modified Grubbs ruthenium initiators. *J. Mol. Catal. A-Chem.* **2004**, *208*, 115–121.

29 Bornand, M.; Chen, P. Mechanism-Based Design of a ROMP Catalyst for Sequence-Selective Copolymerization*Angew. Chem. Int. Edit.* **2005**, *117*, 7909-7911.

30 Lichtenheldt, M.; Wang, D.; Vehlow, K.; Reinhardt, I.; Kuhnel, C.; Decker, U.; Blechert, S.; Buchmeiser, M. Alternating Ring-Opening Metathesis Copolymerization by Grubbs-Type Initiators with Unsymmetrical N-Heterocyclic Carbenes. *Chem-Eur. J.* **2009**, *15*, 9451–9457.

31 Vehlow, K.; Lichtenheldt, M.; Wang, D.; Blechert, S.; Buchmeiser, M. R. Alternating Ring-Opening Metathesis Copolymerization of Norborn-2-ene with *cis* -Cyclooctene and Cyclopentene. *Macromol. Symp.* **2010**, *296*, 44–48.

32 Bornand, M.; Torker, S.; Chen, P. Mechanistically Designed Dual-Site Catalysts for the Alternating ROMP of Norbornene and Cyclooctene. *Organometallics* **2007**, *26*, 3585–3596.

33 Choi, T.-L.; Rutenberg, I. M.; Grubbs, R. H. Synthesis of A,B-Alternating Copolymers by Ring-Opening-Insertion-Metathesis Polymerization. *Angew. Chem. Int. Ed.* **2002**, *41*, 3839–3841.

34 Lee, H.-K.; Bang, K.-T.; Hess, A.; Grubbs, R. H.; Choi, T.-L. Multiple Olefin Metathesis Polymerization That Combines All Three Olefin Metathesis Transformations: Ring-Opening, Ring-Closing, and Cross Metathesis. *J. Am. Chem. Soc.* **2015**, *137*, 9262–9265.

35 Sinclair, F.; Alkattan, M.; Prunet, J.; Shaver, M. P. Olefin cross metathesis and ring-closing metathesis in polymer chemistry. *Polym. Chem.* **2017**, *8*, 3385–3398.

36 Demel, S.; Slugovc, C.; Stelzer, F.; Fodor-Csorba, K.; Galli, G. Alternating Diene Metathesis Polycondensation (ALTMET) – A Versatile Tool for the Preparation of Perfectly Alternating AB Copolymers. *Macromol. Rapid. Comm.* **2003**, *24*, 636–641.

37 Schulz, M. D.; Wagener, K. B. Solvent Effects in Alternating ADMET Polymerization. *ACS Macro. Lett.* **2012**, *1*, 449–451.

38 Abbas, M.; Wappel, J.; Slugovc, C. Alternating Diene Metathesis Polycondensation (ALTMET) – Opitimizing Catalyst Loading. *Macromol. Symp.* **2012**, *311*, 122–125.

39 Gorodetskaya, I. A.; Choi, T.-L.; Grubbs, R. H. Hyperbranched Macromolecules via Olefin Metathesis. *J. Am. Chem. Soc.* **2007**, *129*, 12672–12673.

40 Ding, L.; Xie, M.; Yang, D.; Song, C. Efficient Synthesis of Long-Chain Highly Branched Polymers via One-Pot Tandem Ring-Opening Metathesis Polymerization and Acyclic Diene Metathesis Polymerization. *Macromolecules* **2010**, *43*, 10336–10342.

41 Note that the amount of ethylene released and of the acrylate conversion are not exactly matching. Indeed, the total amount of ethylene formed (*a priori* 100%) is divided into the ethylene released (the one we are considering) and the ethylene involved in a possible reaction with the polymer which gives non-functional chain-end groups. The amount of ethylene released has been herein determined by calculating the difference between the amount of acrylate that reacted (i.e. the amount of ethylene formed = 100%), and the sum of the amount of non-functional chain-end groups in the polymer plus the amount of isomerized chain-end groups (since no benzoquinone was used to prevent isomerization), as determined by ^{1}H NMR analyses.

42 Chauveau, C.; Vanbiervliet, E.; Fouquay, S.; Michaud, G.; Simon, F.; Carpentier, J.-F.; Guillaume, S. M. Azlactone telechelic polyolefins as precursors to polyamides: a combination of metathesis polymerization and polyaddition reactions. *Macromolecules* **2018**, *51*, 8084-8099.

43 Vanbiervliet, E.; Fouquay, S.; Michaud, G.; Simon, F.; Carpentier, J.-F.; Guillaume, S. M. α,ω-Epoxide, oxetane and dithiocarbonate telechelic copolyolefins: access by ring-opening metathesis/cross-metathesis polymerization (ROMP/CM) of cycloolefins in the presence of functional symmetric chain-transfer agents. *Polymers,* **2018**, *10*, 1241-1260.

44 Vanbiervliet, E.; Fouquay, S.; Michaud, G.; Simon, F.; Carpentier, J.-F.; Guillaume, S. M. From Epoxide to Cyclodithiocarbonate Telechelic Polycyclooctene through Chain-Transfer Ring-Opening Metathesis Polymerization (ROMP): Precursors to Non-Isocyanate Polyurethanes (NIPUs), *Macromolecules* **2017**, *50*, 69-82.

45 https://adhesive-resins.evonik.com/product/adhesive-resins/en/products/polyvest/

46 Due to uncontrolled polycondensation reactions observed on some SMP samples during the second cooling step (probably promoted by the high temperature and the condensation

of moisture on the DSC capsule (opened, under a flux of helium) (Figure S27), only the first heating and cooling cycles were herein considered.

[47] Schapman, F.; Couvercelle, J.-P.; Bunel, C. Low Molar Mass Polybutadiene Made Crosslinkable by the Introduction of Silane Moities via Urethane Linkage: 1. Synthesis and Kinetic Study. *Polymer* **1998**, *39*, 965–971.

[48] Schapman, F.; Couvercelle, J.-P.; Bunel, C. Low Molar Mass Polybutadiene Made Crosslinkable by Silane Moities Introduced via Addition of Thiol to Double Bond: 4. Crosslinking Study. *Polymer* **2000**, *41*, 17–25.

[49] Liu, C.; He, J.; van Ruymbeke, E.; Keunings, R.; Bailly, C. Evaluation of different methods for the determination of the plateau modulus and the entanglement molecular weight. *Polymer* **2006**, 47, 4461–447.

[50] Fouquay, S.; Simon, F.; Michaud, G.; Chauveau, C.; Carpentier, J.-F.; Guillaume S. M. Hydrocarbon copolymers with alternating blocks and alkoxysilane end groups. Bostik SA – CNRS – Université de Rennes 1 FR 3087442 A1; WO2020/079370 A1 (2018-10-18).